Article

Immunity

Inflammasome Activation Triggers Caspase-1-Mediated Cleavage of cGAS to Regulate Responses to DNA Virus Infection

Graphical Abstract

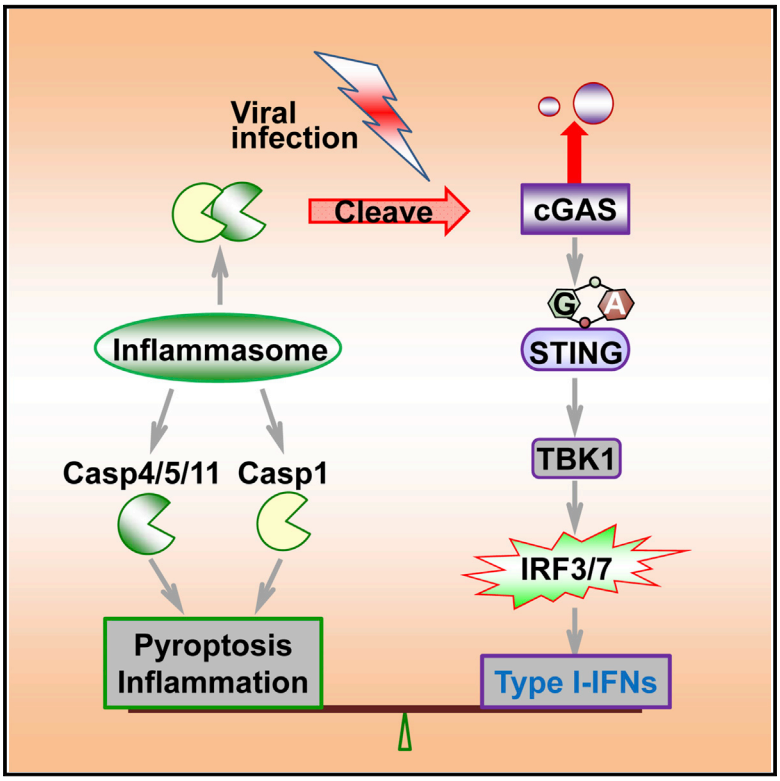

Authors

Yutao Wang, Xiaohan Ning, Pengfei Gao, ..., Guangxun Meng, Xiaodong Su, Zhengfan Jiang

Correspondence

jiangzf@pku.edu.cn

In Brief

Type I interferons (IFN) can inhibit inflammasome activation. Wang et al. find that upon inflammasome activation, inflammatory caspases cleave cGAS and render it inactive. Their findings reveal a role for inflammasomes in the dampening of IFN activating pathways and suggest a double-negative feedback loop that regulates the output of DNA-sensing pathways.

Highlights

- IFN production by *Asc*$^{-/-}$ and *Casp1*$^{-/-}$ macrophages is elevated upon DNA virus infection
- Caspase-1 cuts cGAS during DNA virus infection, but not RNA virus challenge
- Caspase-4, 5, and 11 cut cGAS in conditions of non-canonical inflammasome activation
- cGAS N-terminal R/K-rich region is essential for its physiological function

Wang et al., 2017, Immunity *46*, 393–404
March 21, 2017
http://dx.doi.org/10.1016/j.immuni.2017.02.011

CellPress

Immunity
Article

Inflammasome Activation Triggers Caspase-1-Mediated Cleavage of cGAS to Regulate Responses to DNA Virus Infection

Yutao Wang,[1,2,3,6] Xiaohan Ning,[1,2,3,6] Pengfei Gao,[1,2,3] Shuxian Wu,[4] Mengyin Sha,[1,2,3] Mengze Lv,[1,2,3] Xiang Zhou,[1,2,3] Juyi Gao,[1,2,3] Run Fang,[1,2,3] Guangxun Meng,[4] Xiaodong Su,[1] and Zhengfan Jiang[1,2,3,5,*]
[1]State Key Laboratory of Protein and Plant Gene Research, School of Life Sciences, Peking University, Beijing 100871, China
[2]Key Laboratory of Cell Proliferation and Differentiation of the Ministry of Education, School of Life Sciences, Peking University, Beijing 100871, China
[3]Peking-Tsinghua Center for Life Sciences, Beijing 100871, China
[4]Key Laboratory of Molecular Virology and Immunology, Institut Pasteur of Shanghai, Chinese Academy of Sciences, Shanghai 200031, China
[5]Lead Contact
[6]Co-first author
*Correspondence: jiangzf@pku.edu.cn
http://dx.doi.org/10.1016/j.immuni.2017.02.011

SUMMARY

Viral infection triggers host innate immune responses that result in the production of various cytokines including type I interferons (IFN), activation of inflammasomes, and programmed cell death of the infected cells. Tight control of inflammatory cytokine production is crucial for the triggering of an effective immune response that can resolve the infection without causing host pathology. In examining the inflammatory response of *Asc*$^{-/-}$ and *Casp1*$^{-/-}$ macrophages, we found that deficiency in these molecules resulted in increased IFN production upon DNA virus infection, but not RNA virus challenge. Investigation of the underlying mechanism revealed that upon canonical and non-canonical inflammasome activation, caspase-1 interacted with cyclic GMP-AMP (cGAMP) synthase (cGAS), cleaving it and dampening cGAS-STING-mediated IFN production. Deficiency in inflammasome signaling enhanced host resistance to DNA virus in vitro and in vivo, and this regulatory role extended to other inflammatory caspases. Thus, inflammasome activation dampens cGAS-dependent signaling, suggesting cross-regulation between intracellular DNA-sensing pathways.

INTRODUCTION

Viral infection triggers host antiviral innate immune responses. Cells use different pattern-recognition receptors to detect viral infection by sensing viral nucleic acids (Takeuchi and Akira, 2010). Whereas Toll-like receptor 3 (TLR3) recognizes viral double-stranded RNA (dsRNA) and triggers downstream pathway by TRIF (TIR domain-containing adaptor inducing interferon-β) (Alexopoulou et al., 2001), retinoic acid-inducible gene I (RIG-I)-like helicases (Yoneyama et al., 2004) recognize cytoplasmic viral RNAs, and are transduced by the mitochondrial protein MAVS (VISA, IPS-1, or Cardif) (Kawai et al., 2005; Meylan et al., 2005; Seth et al., 2005; Xu et al., 2005). For cytoplasmic DNA sensing, it has been discovered that cGAS (cyclic GMP-AMP (cGAMP) synthase) (Sun et al., 2013) recognizes cytosolic DNA and produces cGAMP (Ablasser et al., 2013; Civril et al., 2013; Gao et al., 2013; Wu et al., 2013a), which functions as a second messenger to activate STING (stimulator of IFN genes, also named MITA or ERIS) (Ishikawa and Barber, 2008; Sun et al., 2009; Zhong et al., 2008). Additionally, RNA polymerase III (Ablasser et al., 2009; Chiu et al., 2009) serves as another cytoplasmic sensor of DNA by transcribing AT-rich dsDNA into dsRNA, thus stimulating RIG-I-MAVS pathway. Activation of these receptors leads to the activation of transcription factors NF-κB and IFN regulatory factor IRF-3 or IRF-7 and the production of various cytokines including type I-IFNs. Secreted type I-IFNs bind to their receptor and induce the expression of hundreds of interferon-stimulated genes (ISGs), which interfere with almost every step of viral replication, resulting in the establishment of a cellular anti-viral state (Takeuchi and Akira, 2010).

Microbial infection also causes pathological inflammation, which is mediated by the activation of inflammasome complexes, leading to the activation of inflammatory caspases (caspase-1, and caspase-4/5 in human, or caspase-11 in mouse) (Kumar, 2007; McIlwain et al., 2015). Inflammasomes are triggered by Nod-like receptors (NLRs), which recognize microbial products, including viral nucleic acids, or endogenous molecules released from damaged or dying cells (Kanneganti, 2010; Rathinam et al., 2012). Upon activation, NLRs oligomerize and recruit pro-caspase-1, with or without the help of ASC (apoptosis-associated speck-like protein with a caspase-recruitment domain), leading to the activation of caspase-1, and subsequent proteolytic conversion of proinflammatory cytokines, interleukin-1 (IL-1β) and IL-18 from their precursors (Rathinam et al., 2012). AIM2 (absent in melanoma 2) has also been shown to activate ASC-dependent inflammasome in response to cytosolic dsDNA (Fernandes-Alnemri et al., 2009; Hornung et al., 2009). Additionally, either caspase-1 or caspase-11 triggers a form of lytic, programmed cell death called pyroptosis (Jorgensen and Miao, 2015). Interestingly, caspase-1 has been shown to cleave proteins involved in innate immune activation, such as Mal and

TRIF, resulting in reduced cytokine production after bacterial infections because both play essential roles in TLR-mediated signaling (Jabir et al., 2014; Miggin et al., 2007; Ulrichts et al., 2010).

Although type I-IFNs are critical for suppressing the spread of viral infection, aberrant production of these cytokines can have pathological roles in a variety of autoimmune disorders (Crow, 2014; Ivashkiv and Donlin, 2014; Nallar and Kalvakolanu, 2014). Importantly, because microbial infection usually leads to type I-IFN production and inflammasome activation, balance between these key pathways is essential for immune homeostasis. Indeed, it has been reported that rheumatic diseases, for example, is either driven by inflammasome-induced proinflammatory secretion or by abnormal type I-IFN production (van Kempen et al., 2015). Previous work demonstrated that type I-IFNs inhibit inflammasome activation (Guarda et al., 2011) and that various NLRs such as NLRX1 (Lei et al., 2012; Moore et al., 2008), NLRP4 (Cui et al., 2012), NLRP6 (Anand et al., 2012), NLRC3 (Schneider et al., 2012; Zhang et al., 2014), and NLRC5 (Benko et al., 2010; Cui et al., 2010) negatively regulate type I-IFN induction in different ways, highlighting the importance of this fine-tuning regulation.

Here we report that caspases controlled antiviral immunity through cGAS cleavage during inflammasome activation. Upon inflammasome activation, caspase-1 directly bound to and cleaved human cGAS at $D^{140/157}$, resulting in reduced cGAMP production and cytokine expression. Consequently, caspase-1, AIM2- and ASC-deficient mice showed enhanced resistance to infection by DNA but not RNA virus. cGAS was also cleaved by caspase-4, -5, and -11 during non-canonical inflammasome activation, triggered by intracellular lipopolysaccharides (LPS) delivery. Importantly, we also found that cGAS N-terminal R/K-rich region between residues 122 to 133 of human cGAS and residues 119 to 132 of mouse cGAS was critical for its normal function. Our study therefore revealed a role for caspases in the regulation of cGAS-STING pathway and provided molecular insight into the coordination between antiviral innate immune and inflammasome activation. Because numerous caspase inhibitors are under clinical trials, our findings suggested that these inhibitors' potential effect as immune boosters should be closely investigated and efforts should be made to avoid unwanted or excessive innate immune activation caused by these inhibitors.

RESULTS

Asc$^{-/-}$ or *Casp1*$^{-/-}$ Deficiency Augments Cytokine Production and Host Resistance to DNA Virus Infection

In our screening of molecules that regulate virus-triggered innate immune activation, we detected higher type I-IFN, interleukin-6 (IL-6) and TNF production in peritoneal macrophages from either *Asc*$^{-/-}$ or *Casp1*$^{-/-}$ mice than in those from wild-type mice. This increase was observed in response to genomic DNA (gDNA) transfection, as well as DNA virus herpes simplex virus 1 (HSV-1) or Vaccinia virus (VACV) infection, but not to infection by Sendai virus (SeV), an RNA virus (Figures 1A and 1B and S1A). Consistently, the mRNA levels of *Ifna*, *Ifnb*, *Il-6*, *Il-10*, *Il-12*, and some *ISGs* were significantly higher in *Asc*$^{-/-}$ and *Casp1*$^{-/-}$ macrophages transfected with gDNA (Figure S1B). Similarly, the activation of the kinase TBK1 represented by its phosphorylation and the production of Viperin, a well-known ISG (Chin and Cresswell, 2001), were enriched in these deficient cells (Figure 1C). Fluorescent microscopy and flow cytometry analysis showed that compared to WT cells, *Asc*$^{-/-}$ and *Casp1*$^{-/-}$ cells were resistant to HSV-1-GFP infection, whereas all these cells showed similar susceptibility to another RNA virus vesicular stomatitis virus (VSV)-GFP infection (Figures S1C and S1D). These data suggested that ASC and caspase-1 negatively regulate cytosolic DNA, but not RNA triggered innate immune responses in mouse cells.

To confirm this observation in human cells, we performed RNAi of caspase-1 in human acute monocytic leukemia cell line THP-1 by shRNA and studied type I-IFN induction upon viral infection (Lei et al., 2013). When infected with VACV or HSV-1, we could detect visible increases in IRF3 activation and Viperin expression after caspase-1 expression was interfered (*CASP1*^{RNAi}), which were not observed in SeV-infected cells (Figure 1D). Consistently, type I-IFNs were boosted in *CASP1*^{RNAi} cells by HSV-1 or VACV, but not SeV infection (Figure 1E). As a well-known ISG and a critical transcription factor for type I-IFN production, the induction and dimerization of IRF-7 were all stronger in *CASP1*^{RNAi} cells in response to DNA virus (Figure S1E). AIM2 was shown to activate ASC-dependent inflammasome in response to cytosolic dsDNA. We observed similar results as macrophages from *Aim2*$^{-/-}$ mice showed exaggerated responses only to DNA virus (Figures 1F and 1G), which is consistent with previous results (Corrales et al., 2016; Hornung et al., 2009). Since this inflammasome activation led to ASC and caspase-1 activation, these data collectively suggested that ASC and caspase-1 negatively regulated DNA virus-induced type I-IFN production.

We then looked for in vivo evidence. Consistent with the above data, *Casp1*$^{-/-}$ or *Asc*$^{-/-}$ mice were resistant to VACV but not VSV infection compared to the wild-type mice (Figure 1H), which was associated with lower viral loads in the lungs of *Asc*$^{-/-}$ and *Casp1*$^{-/-}$ mice (Figure 1I). Consistently, we detected higher type I-IFN and IL-6 production in the spleens and lungs of *Casp1*$^{-/-}$ or *Asc*$^{-/-}$ mice after VACV infection (Figure 1J) and the increased expression of Viperin in organs from deficient mice (Figure S1F).

Inflammasome Activation Attenuates DNA Virus-Triggered Signaling

Because AIM2, ASC, or caspase-1 deficiency resulted in the elevated innate immune responses to DNA virus, we sought to determine the intrinsic correlation between inflammasome activation and type I-IFN induction. First we confirmed that inflammasomes in THP-1 cells were intact, as the processed IL-1β was detected after LPS plus ATP or rotenone treatment (Figure 2A). Although VACV infection stimulated both IFN and inflammasome activations (Figures 1D and 2A), its ability to induce IRF3 phosphorylation and Viperin expression was almost completely lost when inflammasomes were first induced by either LPS plus rotenone (Figure 2B), LPS plus ATP (Figure 2C), or MALP2 plus ATP (Figure S2A). Consistently, VACV triggered type I-IFN production was lost after inflammasome activation (Figures 2D and 2E and S2A). Similar patterns were found in THP-1 cells infected with HSV-1 (Figures 2B and 2D and data not shown), but not in those infected with RNA virus SeV (Figure S2B). These data suggest that enforced inflammasome

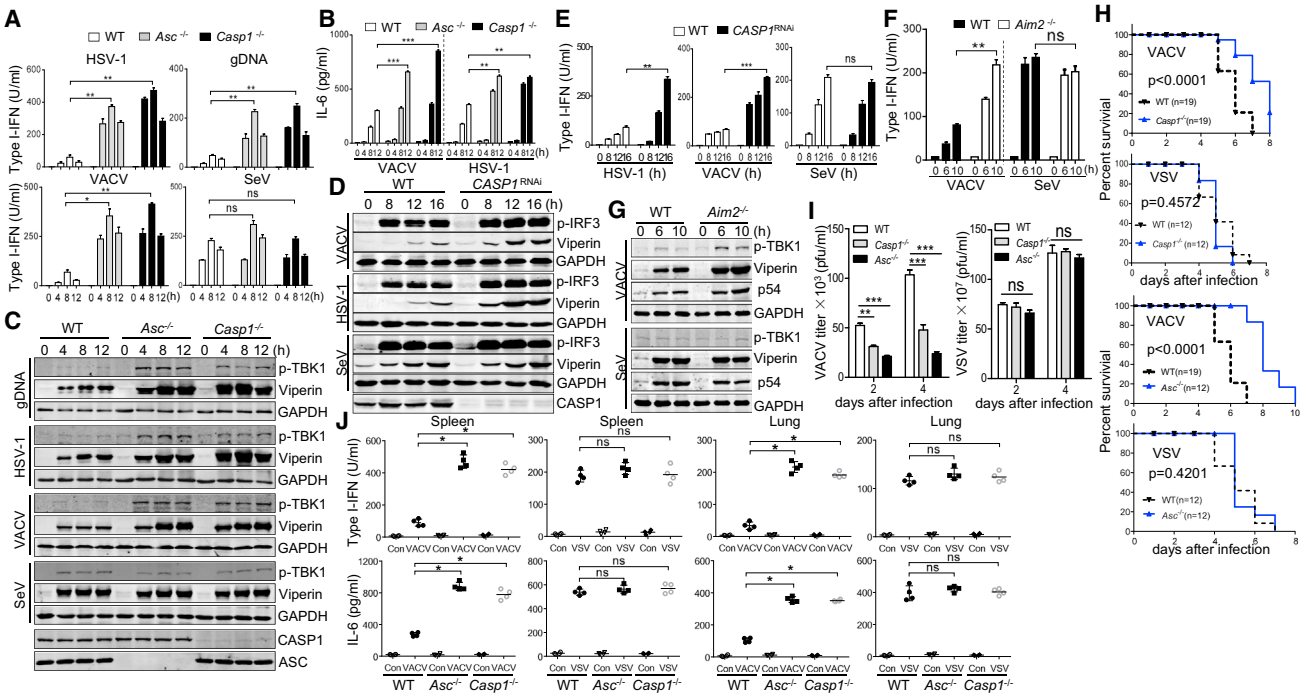

Figure 1. Inflammasome Defect Augments Cytokine Production and Host Resistance to DNA Virus Infection

(A) WT, *Asc*$^{-/-}$, and *Casp1*$^{-/-}$ peritoneal macrophages were left untreated or stimulated with VACV, HSV-1, SeV, or gDNA for the indicated times. Supernatants were analyzed by type I-IFN bioassay. gDNA, Calf thymus genomic DNA.

(B) WT, *Asc*$^{-/-}$, and *Casp1*$^{-/-}$ peritoneal macrophages were left uninfected or infected with VACV or HSV-1 for the indicated times. Supernatants were collected for quantization of IL-6 cytokine by ELISA.

(C) Cell lysates in (A) were analyzed by immunoblotting with the indicated antibodies.

(D and E) Casp1-shRNA stably transfected THP-1 cells (*CASP1*^{RNAi}) were infected with VACV, HSV-1, or SeV for the indicated times. Cell lysates were analyzed by immunoblotting (D) and supernatants were analyzed by type I-IFN bioassay (E).

(F and G) WT and *Aim2*$^{-/-}$ peritoneal macrophages were infected with VACV or SeV for the indicated times and analyzed by type I-IFN bioassay (F) and immunoblotting (G).

(H) WT, *Asc*$^{-/-}$, and *Casp1*$^{-/-}$ mice were infected intranasally (i.n.) with VACV at 3 × 10^6 pfu per mouse or intravenously (i.v.) with VSV at 2 × 10^7 pfu per mouse, and the survival rates of mice were observed and recorded for 2 weeks.

(I) WT, *Asc*$^{-/-}$, and *Casp1*$^{-/-}$ mice (n = 4) were infected as indicated in (H), and lungs were harvested 2 and 4 days later for viral load measurement.

(J) WT, *Asc*$^{-/-}$ or *Casp1*$^{-/-}$ mice (n = 4) were infected i.v. with VACV at 3 × 10^6 pfu per mouse or VSV at 2 × 10^7 pfu per mouse for 8 hr before cytokines production in organs were measured.

*p < 0.05, **p < 0.01, ***p < 0.001, ns p > 0.05. Values are mean ± SEM. Data are representative of three independent experiments.

See also Figure S1.

activation attenuates DNA virus-induced type I-IFN production in human cells. To confirm whether this phenomenon was also true for mouse cells, we used immortalized bone-marrow-derived macrophages (iBMM), which harbor both inflammasome (Figure 2F) and type I-IFN pathways. Inflammasome activation restrained VACV-induced type I-IFN activation, as measured by TBK1 phosphorylation, Viperin, and type I-IFN production (Figures 2G and S2C). Inflammasome activation also causes pyroptotic cell death, which would possibly diminish type I-IFN production. However, because the induced inflammasome activation didn't affect RNA virus-induced type I-IFN production, we reasoned that caspase-1-mediated pyroptotic cell death might not be essential role in this process. To confirm this, GSDMD-deficient iBMM cells, which are resistant to caspase-1/11-mediated pyroptosis (Kayagaki et al., 2015; Shi et al., 2015), were pretreated with LPS plus ATP or rotenone, followed by VACV or SeV infection. We found that DNA virus-triggered type I-IFN production, Viperin or p54 induction was also severely reduced in *Gsdmd*$^{-/-}$ cells after inflammasome activation (Figures S2D and 2H). Moreover, cells were also tested with the synthetic triggers of cGAS (dsDNA) and RNA sensors (poly(I:C)). The results were consistent with viral infection in both mouse and human cells, as inflammasome-activated cells showed reduced response to poly(dAdT), but not to poly(I:C) (Figures S2E and S2F). Together, these data suggest that inflammasome activation attenuates DNA virus-induced type I-IFN production.

Caspase Inhibitors Potentiates DNA Virus-Triggered Signaling

To determine whether the pharmacological inhibition of caspase could recapitulate the phenotype caused by genetic deficiencies, we used caspase-1-specific inhibitor VX765, which blocked IL-1β processing (Figure 3A) and caspase-1 activation (Figure 3B). This inhibitor caused a highly increased expression

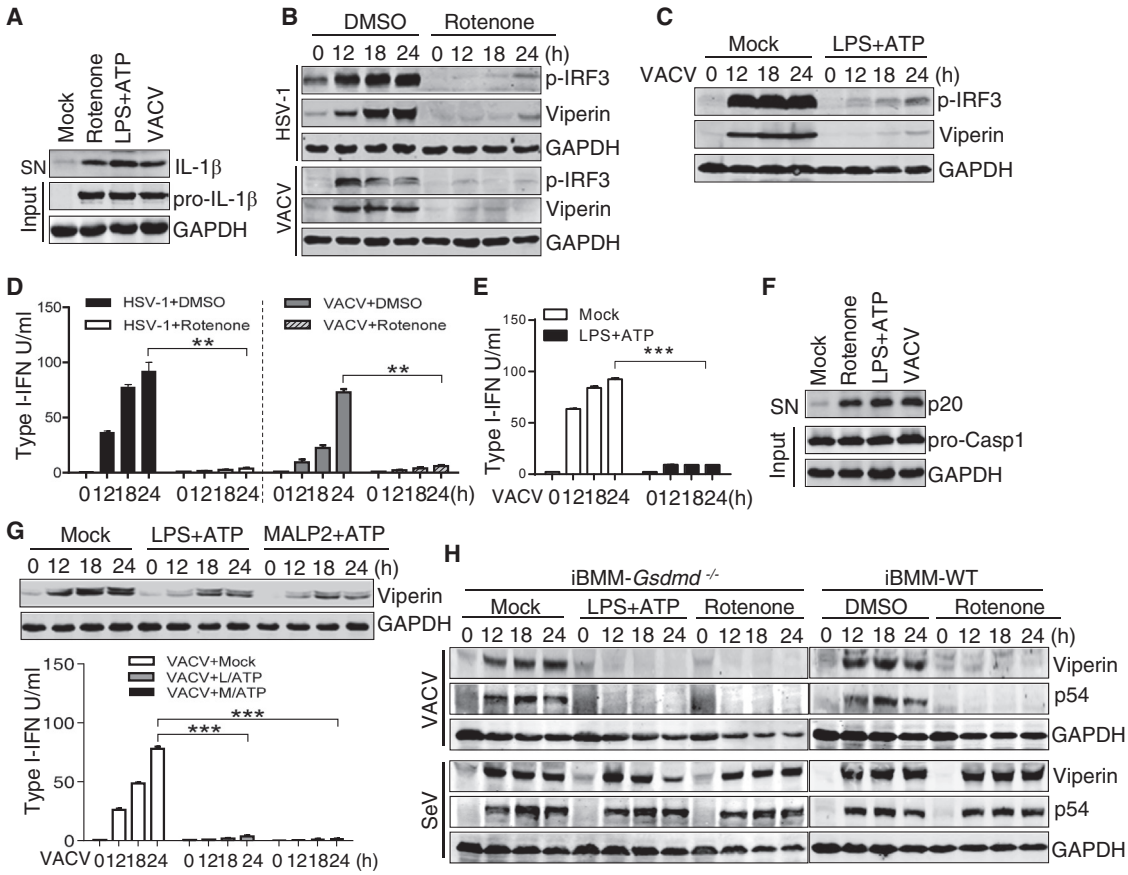

Figure 2. Inflammasome Activation Attenuates DNA Virus-Triggered Signaling

(A) LPS primed THP-1 cells were treated with rotenone, ATP, or VACV. Supernatants (SN) and cell lysates (Input) were analyzed by immunoblotting.

(B–E) THP-1 cells were left untreated or pretreated with LPS plus rotenone (B) or ATP (C), and then infected with HSV-1 or VACV for the indicated times. Cell lysates were analyzed by immunoblotting and supernatants were subjected to type I-IFN bioassay (D and E).

(F) LPS primed iBMM cells were stimulated with rotenone, ATP, or VACV before supernatants (SN) and cell extracts (Input) were analyzed by immunoblotting.

(G) iBMM cells were left untreated or pretreated with LPS or MALP2 plus ATP, and then infected with VACV for the indicated times followed by immunoblotting analysis and type I-IFN bioassay.

(H) iBMM-*Gsdmd*$^{-/-}$ cells or iBMM-WT cells were left untreated or pretreated with LPS plus ATP or rotenone, and then infected with VACV or SeV for the indicated times followed by immunoblotting analysis.

**p < 0.01 and ***p < 0.001. Values are mean ± SEM. Data are representative of three independent experiments.

See also Figure S2.

of Viperin and enhanced IRF3 phosphorylation upon VACV infection (Figure 3C). Meanwhile, no change was found for SeV infection. Similarly, Viperin expression and type I-IFN production were increased in mouse peritoneal macrophages (Figure 3D) or iBMMs treated with VX765 (Figure S3A). Importantly, while pre-induced inflammasome activation severely impaired VACV-triggered type I-IFN and Viperin production, the same pre-treatment on *Casp1*$^{-/-}$ (Figure 3E) or *Asc*$^{-/-}$ (Figure S3B) cells had no effect. Similar results were obtained in *CASP1*^{RNAi} cells (Figures S3C and S3D). These data strongly suggested that inflammasomes-induced innate immune suppression was mediated by caspase-1. Interestingly, when THP-1 cells were treated with z-VAD-fmk, a broad-spectrum inhibitor of caspases, it induced enhanced IRF3 phosphorylation and Viperin expression (Figure 3F), as well as type I-IFN production (Figure 3G) to both RNA and DNA virus infection.

cGAS Is Recruited to and Cleaved by Caspase-1 during Canonical Inflammasome Activation

Cytosolic dsDNA triggers cGAS to synthesize cGAMP, which activates STING. Because caspase-1 is essential to suppress DNA virus-induced antiviral immunity, we hypothesized that caspase-1 exerted its effect on either cGAS or STING. We therefore tested protein interaction between caspase-1 and cGAS or STING and found that caspase-1 interacted with cGAS, but not with STING (Figure 4A). Critically, this interaction was greatly enhanced by viral infection or inflammasome activation. Similar results were obtained in iBMM cells (Figure 4B). To determine which domain of caspase-1 interacts with cGAS, we incubated cell lysates containing Flag-tagged Casp1 or its truncations with purified cGAS protein. We found that cGAS interacted directly with caspase-1 and that this interaction required caspase-1 p20 fragment (Figure 4C). Interestingly, we repeatedly observed that cGAS protein

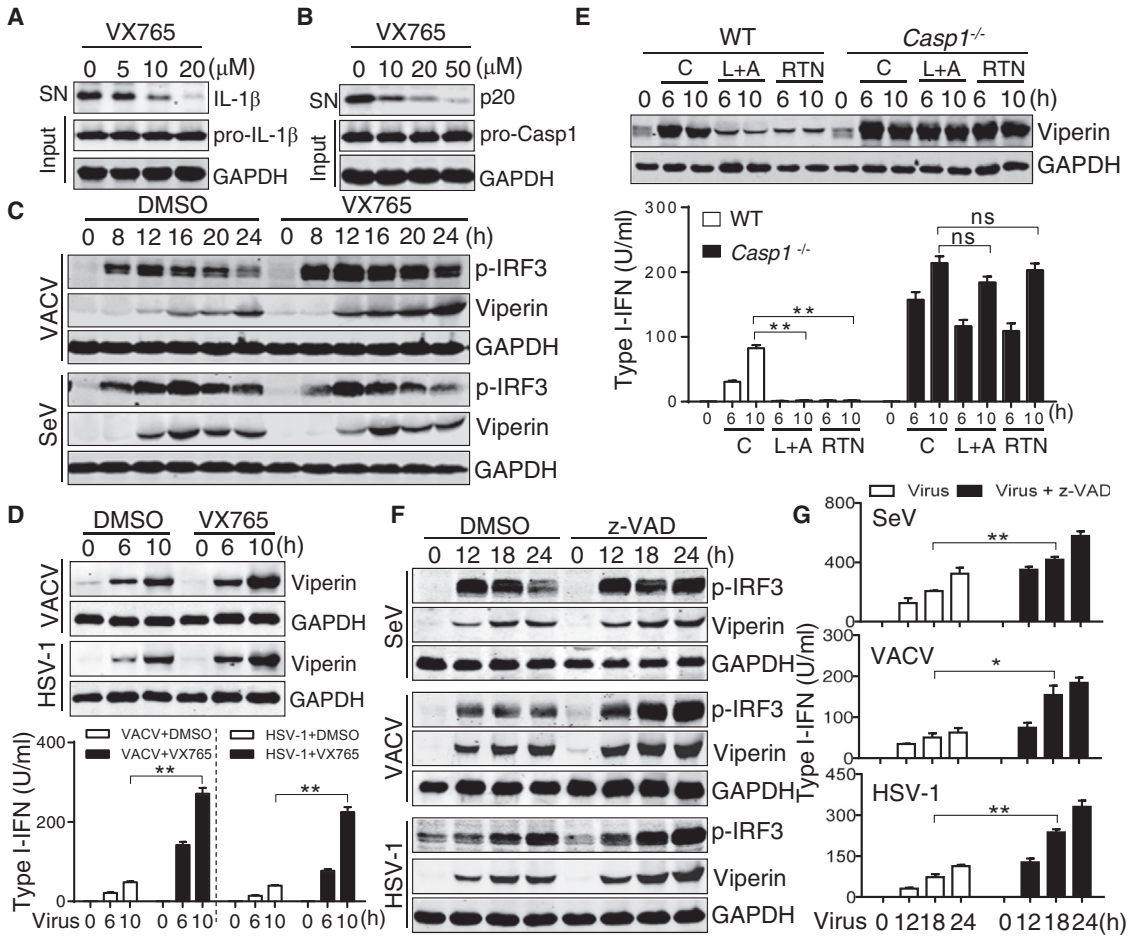

Figure 3. Inflammasome Inhibition Potentiates DNA Virus-Triggered Signaling

(A and B) THP-1 (A) or iBMM cells (B) were pretreated with different doses of VX765 for 2 hr, and then infected with VACV for 18 hr before supernatants (SN) and cell lysates (Input) were analyzed by immunoblotting.

(C) THP-1 cells were left untreated or pretreated with VX765 (20 μM), and then infected with VACV or SeV for the indicated times before immunoblotting analysis.

(D) WT peritoneal macrophages were left untreated or pretreated with VX765 (50 μM), and then infected with VACV or HSV-1 for the indicated times followed by immunoblotting analysis and type I-IFN bioassay.

(E) WT and *Casp1*$^{-/-}$ peritoneal macrophages were left untreated or treated with LPS plus ATP, or rotenone, and then infected with VACV for the indicated times followed by immunoblotting analysis and type I-IFN bioassay. L+A, LPS plus ATP; RTN, rotenone.

(F and G) THP-1 cells were left untreated or pretreated with z-VAD (20 μM) for 2 hr, and then infected with SeV, VACV, or HSV-1 for the indicated times followed by immunoblotting analysis (F) and type I-IFN bioassay (G).

*$p < 0.05$, **$p < 0.01$ ns $p > 0.05$. Values are mean ± SEM. Data are representative of three independent experiments.

See also Figure S3.

was diminished after virus infection or inflammasome activation (Figures 4A, 4B, and S4A). This induced cGAS loss persisted when cellular proteasome and lysosomal pathways were inhibited by MG132 plus Chloroquine (Figure 4D, MG+Chl), but was reversed when caspase-1 inhibitor was used (Figure 4D) or caspase-1 expression was suppressed by shRNA (Figure 4E). Because caspase-1 has been shown to cleave various proteins, like Mal and TRIF, we reasoned that caspase-1 might interact with and cleave cGAS.

To prove this hypothesis, we incubated immunoprecipitation (IP) purified human cGAS (h-cGAS) from 293T cells with bacterially purified caspase-1 and analyzed by western blot. A clear band representing the cleaved cGAS, with a molecular weight 15–20 kDa smaller than the control protein was observed (Figure S4B). Because purified cGAS was C-terminal Flag-tagged, this result indicated that caspase-1 cut cGAS at N terminus. cGAS cleavage did not occur when enzymatic mutant caspase-1 or VX765 was used (Figure S4C). On the contrary, STING or IRF3 protein was not cleaved by caspase-1 (Figures S4A and S4D). We also used N-terminal 3 × Flag- and C-terminal GFP-tagged h-cGAS to monitor the cleavage of cGAS. Both LPS + ATP (Figure 4F) and virus infection (Figure 4G) caused obvious cGAS cleavage. In addition to the major C-terminal fragment detected by anti-GFP antibody (Figures 4F and 4G, indicated as GFP), an N-terminal fragment recognized by anti-Flag antibody with a molecular weight around 20 kDa was also found (Figures 4F and 4G, indicated as Flag), confirming the cleavage of cGAS at the N terminus. Mouse cGAS (m-cGAS) was similarly cleaved

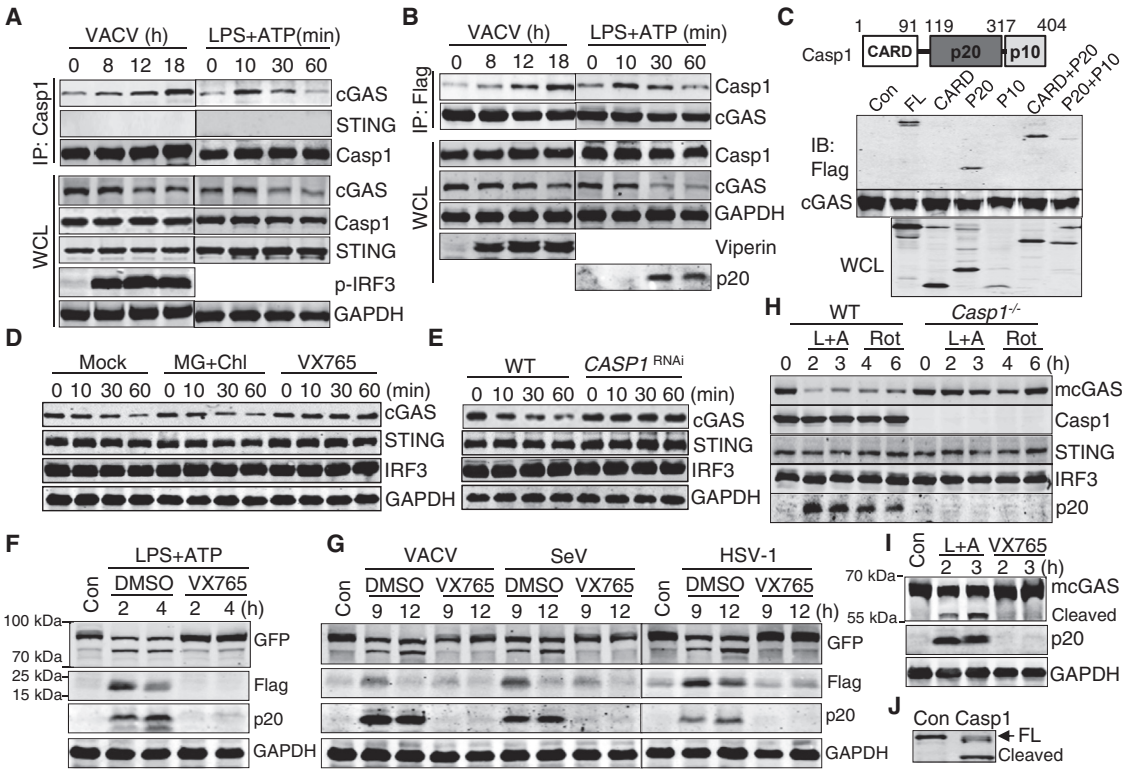

Figure 4. cGAS Is Recruited and Cleaved by Caspase-1 during Inflammasome Activation

(A and B) THP-1 (A) or iBMM cells stably expressed Flag-tagged cGAS (B) were infected with VACV or treated with LPS plus ATP for the indicated times followed by endogenous coimmunoprecipitation and immunoblotting analysis as indicated. WCL, whole cell lysates.

(C) 293T cells were transfected with Flag-tagged caspase-1 (FL) or the indicated truncations for 24 hr followed by in vitro cGAS-GST pull down assay and immunoblotting analysis.

(D) LPS primed THP-1 cells were pretreated with CHX (10 μg/ml) for 1 hr, and then MG132 (25 μM) + Chloroquine (25 μM) or VX765 (20 μM) for 2 hr, followed by ATP treatment for the indicated times before immunoblotting analysis.

(E) LPS primed WT and *CASP1*^{RNAi} THP-1 cells were treated with ATP for indicated times followed by immunoblotting analysis.

(F and G) iBMM cells stably expressing N-terminal-Flag-tagged and C-terminal-GFP-tagged cGAS (Flag-cGAS-GFP) were pretreated with or without VX765, and then stimulated with LPS plus ATP (F), VACV, SeV, or HSV-1 (G) for the indicated times followed by immunoblotting analysis.

(H) WT and *Casp1*$^{-/-}$ BMDMs were pretreated with CHX (10 μg/ml) for 1 hr, followed by LPS plus ATP or rotenone for the indicated times followed by immunoblotting analysis.

(I) LPS primed iBMM cells were pretreated with CHX (10 μg/ml) for 1 hr, and then left untreated or treated with VX765, followed by ATP stimulation for the indicated times. Cell lysates were analyzed by immunoblotting. L+A, LPS+ATP; VX765, LPS+ATP+VX765.

(J) 293T cells were transfected with C-terminal Flag-tagged and N-terminal HA-tagged mcGAS for 24 hr. Cell extracts were coimmunoprecipitation with anti-Flag antibody, followed by in vitro protease cleavage assay and immunoblotting analysis.

Data are representative of three independent experiments.

See also Figure S4.

by caspase-1. Both LPS + ATP and LPS + rotenone caused cGAS disappearance in wild-type, but not *Casp1*$^{-/-}$ BMDMs (bone marrow derived macrophages) (Figure 4H). The cleaved m-cGAS fragment was detected in cells treated with LPS plus ATP (Figure 4I) or infected with VACV or HSV-1 (Figure S4E) and was further blocked by the caspase-1 inhibitor. Moreover, IP-purified m-cGAS was cut by caspase-1 in vitro (Figure 4J).

Caspase-1 Cleaves Human cGAS at D^{140} and D^{157} after Inflammasome Activation

To identify the exact cleavage sites of h-cGAS by caspase-1, we generated cGAS deficient HeLa cells using CRISPR-Cas9 system. HeLa cells were found to have excellent responses to either gDNA or DNA virus when cultured in lower concentrations of Fetal bovine serum (Figure S5A and manuscript in preparation). cGAS deletion led to complete loss of dsDNA-induced IRF3 phosphorylation (Figures S5B and S5C) and type I-IFN production (Figure S5D), whereas cGAS reconstitution restored the responses (Figure S5C). This cGAS-deficient HeLa cell was then used to scrutinize the actual target(s) on h-cGAS. Because deletion of cGAS N-terminal 160 residues (cGAS-dN) does not affect cGAS activation when overexpressed in 293T cells (Sun et al., 2013), we first tested whether cGAS-dN would still be cleaved. iBMM cells stably expressing Flag-cGAS-dN-GFP were infected with VACV or SeV, cGAS cleavage was determined by western blot. There was no cleaved bands appeared (Figure 5A), indicating that caspase-1 cut h-cGAS within the N terminus. Human cGAS contains six aspartic acids in this area, namely

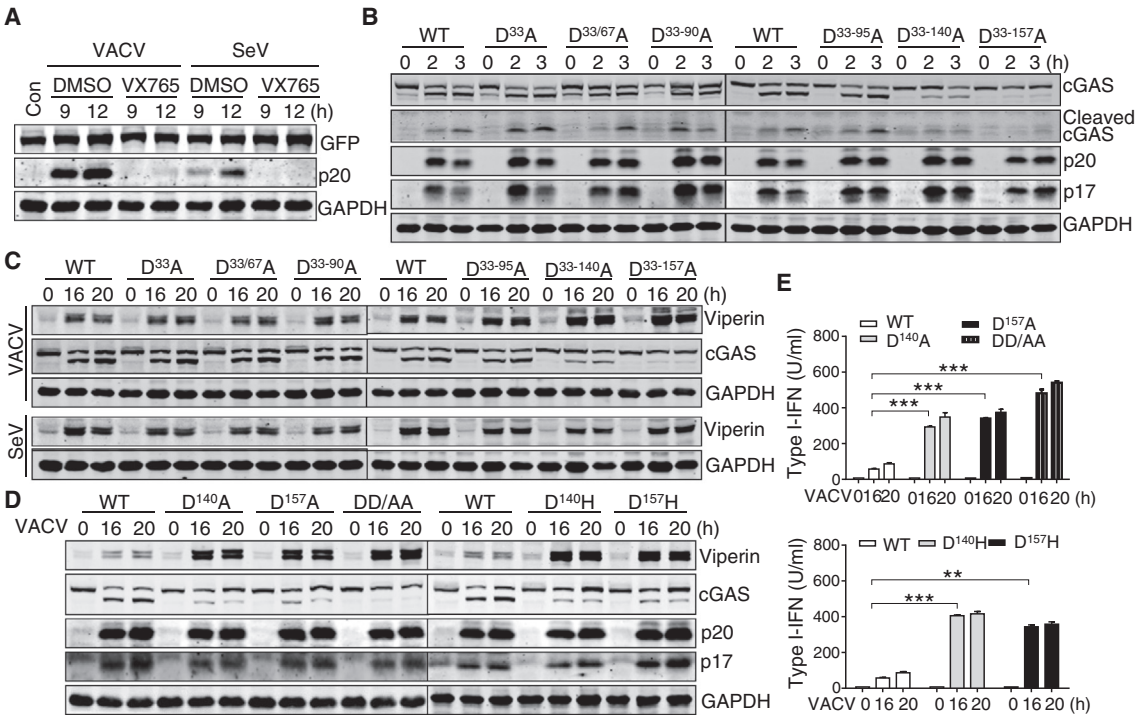

Figure 5. Caspase-1 Cleaves Human cGAS at D^{140} and D^{157} after Inflammasome Activation

(A) iBMM cells stably expressed Flag-cGAS (d6-160aa)-GFP were left untreated or pretreated with VX765, and then infected with VACV or SeV for the indicated times followed by immunoblotting analysis.

(B and C) LPS primed iBMM cells stably expressed WT cGAS or series of cGAS point mutations were stimulated with ATP (B) or infected with VACV or SeV (C) for the indicated times followed by immunoblotting analysis. D^{33}A; D^{33-67}A, $D^{33/67}$A; D^{33-90}A, $D^{33/67/90}$A; D^{33-95}A, $D^{33/67/90/95}$A; D^{33-140}A, $D^{33/67/90/95/140}$A; D^{33-157}A, $D^{33/67/90/95/140/157}$A.

(D and E) iBMM cells stably expressing cGAS-WT, cGAS-D^{157}A/H, cGAS-D^{140}A/H, or cGAS-$DD^{140/157}$AA were infected with VACV for the indicated times followed by immunoblotting analysis (D) and type I-IFN bioassay (E).

**p < 0.01, ***p < 0.001. Values are mean ± SEM. Data are representative of three independent experiments.

See also Figure S5.

D^{33}, D^{67}, D^{90}, D^{95}, D^{140}, and D^{157}, as potential attacking sites for caspase-1 protease. We substituted these aspartic acids by alanine one after another. These cGAS mutants were first shown to activate type I-IFN production when overexpressed (Figure S5E), and then individually stably-expressed in HeLa-*cGAS*$^{-/-}$ cells. When these cells were infected with VACV, we found that each of these cGAS mutant potently activated IRF3 and type I-IFN production (Figure S5F). Because there is no intact inflammasome activation pathway in HeLa cells, each cGAS mutant was individually expressed in iBMM cells and followed by cleavage test. It was found that D^{33-140}A cGAS started to show resistance to caspase-1 cleavage. Replacement of all six aspartic acids (D^{33-157}A) completely abrogated the cleavage (Figure 5B). Consistently, cells expressing D^{33-140}A or D^{33-157}A showed much enhanced responses to DNA virus, accompanied with impaired or loss of cGAS cleavage (Figures 5C and S5G). When individual aspartic acid was mutated, we found that replacement of either D^{140} or D^{157} with alanine (D^{140}A, D^{157}A) or with histidine (D^{140}H, D^{157}H) substantially inhibited viral infection-induced cGAS cleavage. The combined mutation (DD/AA) completely blocked the cleavage (Figure 5D). In agreement with this, cells expressing the mutated cGAS produced more type I-IFNs and ISGs upon DNA virus infection (Figures 5D and 5E and data not shown). Again, overexpression of these mutants in 293T cells all led to strong type I-IFN activation (Figure S5H). Similarly, caspase-1 was also found to target m-cGAS at N terminus (Figure S5I and data not shown). Deletion of the N-terminal residues (m-cGAS-d6-165) blocked the cleavage. These data collectively demonstrated that caspase-1 targeted h-cGAS at D^{140} and D^{157}.

Cleavage of cGAS by Caspase-1 Impairs cGAMP Production

Next, we tested whether cGAS cleavage would affect cGAMP production. We purified cGAMP from VACV-infected THP-1 cells and found that when inflammasomes were first activated, VACV infection triggered cGAMP production was severely impaired as shown by the reduced IRF3 phosphorylation (Figure 6A). Although cGAMP in culture medium induced Digiton-permeabilized THP-1 cells to produce Viperin and type I-IFN (Figures S6A and S6B), this was not affected by inflammasome activation (Figure 6B). Similar results were found in iBMM cells (Figure S6C). These results suggested that inflammasome activation impaired cGAMP production. On the contrary, VACV triggered type I-IFN induction in THP-1 cells was vividly potentiated when caspase-1 was inhibited by VX765 (Figure S6D). Consistently, peritoneal

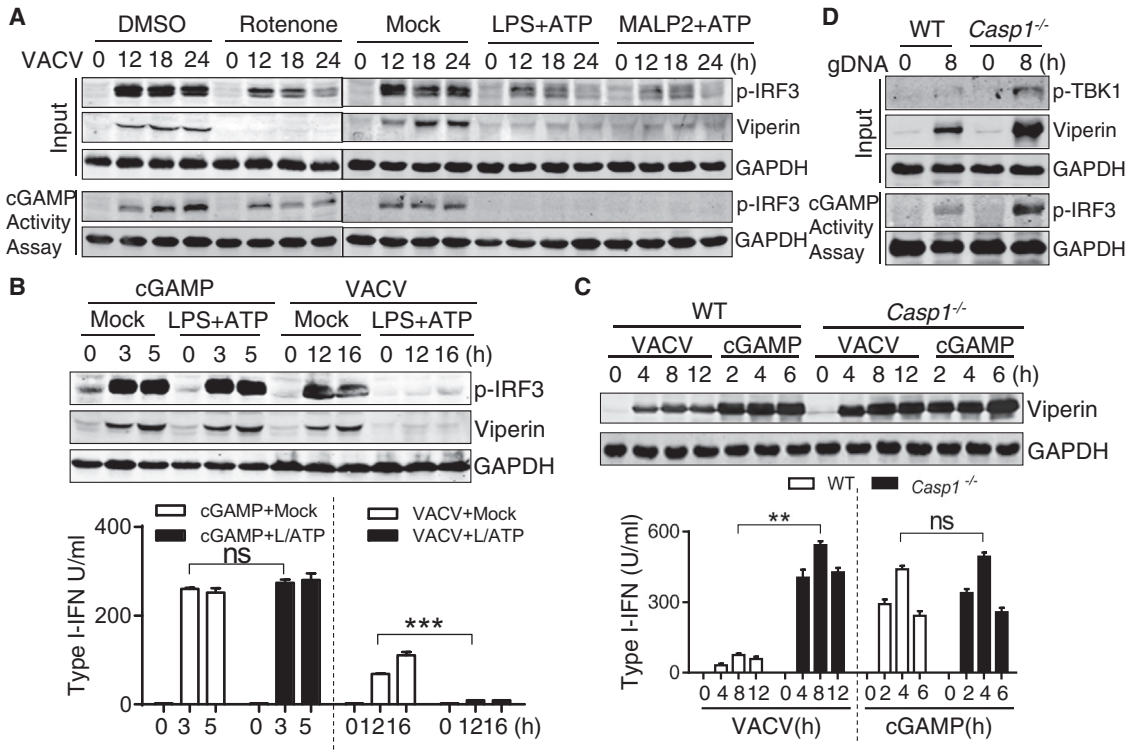

Figure 6. Cleavage of cGAS by Caspase-1 Impairs cGAMP Production

(A) LPS or MALP2 primed THP-1 cells were left untreated or pretreated with rotenone or ATP, and then infected with VACV for the indicated times. cGAMP was purified from the infected cells followed by in vitro cGAMP activity assay and immunoblotting analysis.

(B) THP-1 cells were left untreated or pretreated with LPS plus ATP, and then stimulated with cGAMP (0.1 μg/ml) by digitonin-mediated direct delivery or infected with VACV for the indicated times followed by immunoblotting analysis and type I-IFN bioassay.

(C) WT and *Casp1*$^{-/-}$ peritoneal macrophages were infected with VACV or treated with cGAMP (0.1 μg/ml) by digitonin-mediated direct delivery for the indicated times followed by immunoblotting analysis and type I-IFN bioassay.

(D) WT or *Casp1*$^{-/-}$ BMDMs were left untreated or transfected with gDNA for 8 hr. Cell extracts containing cGAMP were delivered to PFO-permeabilized HeLa-*cGAS*$^{-/-}$ cells for in vitro cGAMP activity assay. PFO, perfringolysin O.

**p < 0.01, ***p < 0.001, ns p > 0.05. Values are mean ± SEM. Data are representative of three independent experiments.

See also Figure S6.

macrophages (Figure 6C) and BMDM (Figure 6D) from *Casp1*$^{-/-}$ mice produced more cGAMP. Altogether, these data showed that active caspase-1 dampened cellular cGAMP production.

cGAS Is Cleaved by Other Pyroptotic Caspases during Non-canonical Inflammasome Activation

In addition, we noticed that the protein level of cGAS was reduced after LPS was delivered into HeLa or iBMM cells (Figure S7A), during which process the non-canonical inflammasome caspases, caspase-11 in mouse and caspase-4 and -5 in human, were activated (Shi et al., 2014). We then tested whether these pyroptotic caspases could also cleave cGAS. Consistent with the cGAS loss in cells treated with LPS, bacterially purified caspase-4, -5, or -11 all cleaved cGAS protein in vitro. Caspase-4 and -11 cleaved cGAS in relatively the same pattern with multiple cleaved bands (Figure S7B), indicating the multiple target sites. When overexpressed cGAS was purified and incubated with active caspase-1, -4, or -11, it was confirmed that caspase-4 and -11 cut cGAS differently compared to caspase-1 (Figure S7C). Again, these caspases only cleaved cGAS, but not STING, TBK1, or IRF3. Caspase-5 also cut cGAS in a different pattern (Figure S7D), in which DD/AA mutation had no effect (Figure S7E). These data collectively suggested that cGAS was cleaved by all inflammatory caspases during either canonical or non-canonical inflammasome activation.

cGAS N terminus Is Critical for Antiviral Innate Immune Activation

Our findings that h-cGAS was cleaved by caspase-1 at $D^{140/157}$ during inflammasome activation and that this cleavage led to the loss of cGAS function are inconsistent with the previous results suggesting that h-cGAS N-terminal 160 residues is dispensable for cGAS function (Sun et al., 2013). To address this discrepancy, we first confirmed that overexpression of either full-length or h-cGAS-dN in 293T cells indeed activated type I-IFN production (Figure S7F). However, when h-cGAS-dN was reconstituted in HeLa-*cGAS*$^{-/-}$ cells, cell response to DNA virus was completely lost (Figures 7A and 7B). This result suggested that cGAS N terminus actually plays a critical role under physiological conditions. To examine which region of this area was important, we generated a series of deletions in this region. We found that whereas deletion of the first 120 amino acids of cGAS did not

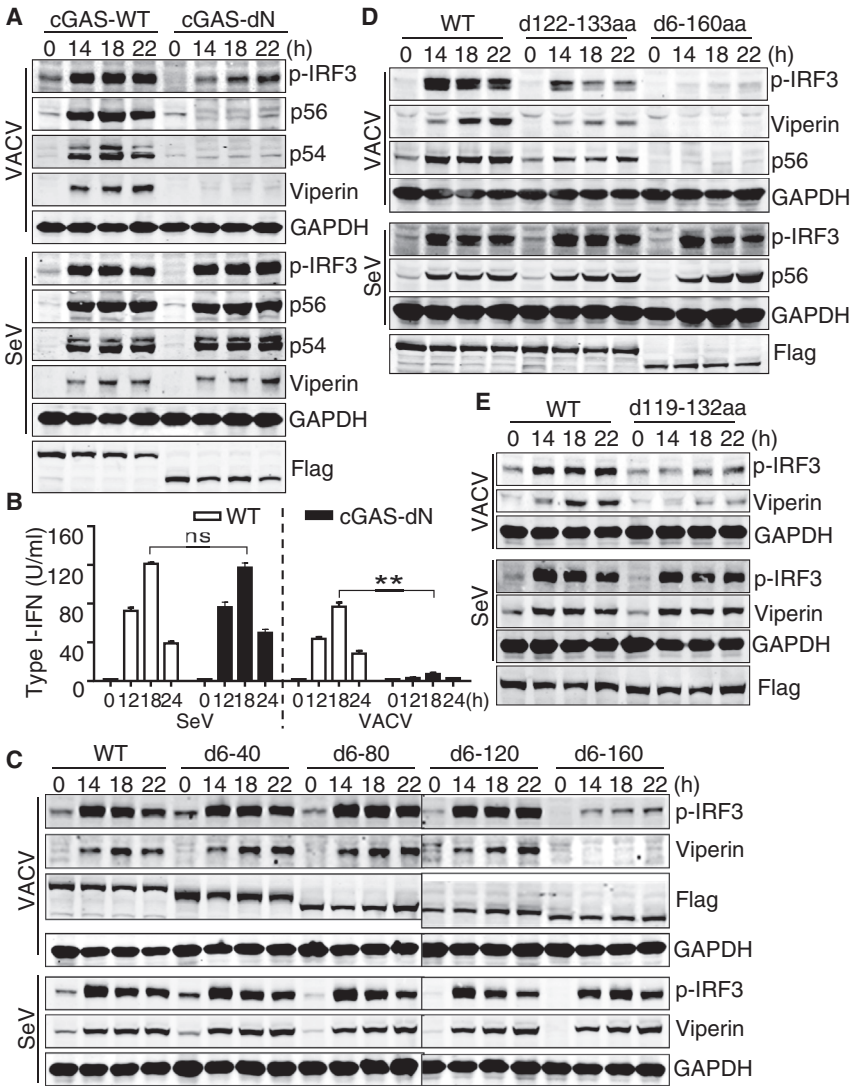

Figure 7. N terminus of cGAS Is Critical for Antiviral Innate Immune Activation

(A and B) HeLa-*cGAS*$^{-/-}$ cells reconstituted with hcGAS-WT or hcGAS-d6-160aa were infected with SeV or VACV for the indicated times followed by immunoblotting analysis (A) and type I-IFN bioassay (B).

(C and D) HeLa-*cGAS*$^{-/-}$ cells reconstituted with hcGAS-WT or the indicated deletions were infected with SeV or VACV for the indicated times followed by immunoblotting analysis.

(E) HeLa-*cGAS*$^{-/-}$ cells reconstituted with mcGAS-WT or mcGAS-d119-132aa were infected with SeV or VACV for the indicated times followed by immunoblotting analysis.

**p < 0.01, ns p > 0.05. Values are mean ± SEM. Data are representative of three independent experiments.

affect its function, further deletion to residue 160 totally abolished cGAS activity (Figure 7C), suggesting the importance of residues 120 to 160. Previous work showed that h-cGAS N terminus is able to bind DNA in vitro. In fact, we found that residues 122 to 133 of h-cGAS and residues 119 to 132 of m-cGAS have a cluster of amino acid R and K (Figure S7G, italic and underlined), positively charged residues important for protein-DNA interaction. This R/K-rich region might thus serve as a DNA binding domain. Deletion analyses revealed that this region was indeed essential for cGAS activation in both human and mouse cells (Figures 7D and 7E).

DISCUSSION

Although caspases have been ascribed to a number of functions in addition to their classical ones in apoptosis and inflammation (McIlwain et al., 2015), their roles in modulating the balance between type I-IFN and inflammasomes have not been thoroughly studied. In this study, we observed that mice lacking AIM2, ASC, or caspase-1 and -11 had enhanced resistance to DNA virus, and that inflammasome negatively regulated antiviral responses by caspase-mediated cGAS cleavage. Because so far only intracellular LPS was known to be recognized by caspase-11 (Shi et al., 2014) and DNA virus infection activated inflammasome through AIM2-ASC-caspase-1 pathway (Fernandes-Alnemri et al., 2009; Rathinam et al., 2010), we concluded that DNA virus-induced hyperresponsiveness in caspase-1and -11 deficient cells or mice was ascribed to the loss of caspase-1. We further demonstrated that caspase-1 directly bound to cGAS through its p20 domain, cleaved h-cGAS at $D^{140/157}$. Similarly, caspase-4 and -5 in human and caspase-11 in mouse were also capable of cGAS cleavage in LPS-induced non-canonical inflammasome activation, though the precise target sites need further investigation. Importantly, the cGAS protein level was severely reduced only after LPS was delivered into cells without caspase inhibitor z-VAD. These results collectively suggested that inflammasome and pyroptosis fine-regulates innate immunity through caspases. Previous work demonstrates that various NLRs negatively regulate type I-IFN induction. NLRC3 is found to interact with both STING and TBK1 to impede STING-TBK1 interaction (Zhang et al., 2014). NLRP4 promotes TBK1 ubiquitination and degradation (Cui et al., 2010). Notably, recent work has also provided some evidence showing that inflammasomes regulate gut microbiota in mice (Levy et al., 2015; Man et al., 2016), and inflammasome defect has been associated with pathologic alterations in gut microbiota, resulting in increased susceptibility to colitis and tumorigenesis (Chen, 2016). Because mice with different genotypes were kept separately in our experiments, the contribution of gut microbiota to the observed phenotype cannot be ruled out, which needs to be clarified in future studies.

Caspase-dependent apoptosis is unique in its capacity to induce a noninflammatory type of cell death (Tait et al., 2014).

Recently it has been reported that caspase-3 and -7 are essential for suppressing apoptosis-triggered cGAS-STING activation, although its molecular basis was unknown (Rongvaux et al., 2014; White et al., 2014). Here we identified a similar regulation in which caspase-1 was critical for limiting cytosolic DNA-induced cGAS-STING activation. These results supported the previous observation that aberrant production of type I-IFN has pathological roles in various autoimmune disorders. Importantly, several pharmacological caspase inhibitors have undergone clinical trials. Our findings indicated that these inhibitors might also cause unwanted immune responses, which might be detrimental to patients in some cases. This kind of side-effects should thus be under close investigation during the clinical trials. Moreover, our study indicated that caspase inhibitors might have the potentials to be used as candidates for antiviral drugs since their abilities to boost innate immune responses.

Evidence also indicates the importance of type I-IFNs in suppressing inflammasome. Type I-IFNs are reported to inhibit NLRP1- and NLRP3-activated inflammasome via STAT1. Type I-IFN- induced IL-10 signals via STAT3 to reduce pro-IL-1α/β production (Guarda et al., 2011; Mayer-Barber et al., 2011). Numerous studies have shown that type I-IFNs are successfully used in the clinic for the treatment of diseases such as multiple sclerosis (Benveniste and Qin, 2007; Billiau, 2006). In addition, IFN treatment has also been used to treat Behcet's syndrome and familiar Mediterranean fever, two inflammatory disorders with IL-1 overproduction (Kötter et al., 2004; Tweezer-Zaks et al., 2008). These findings reveal a frequent crosstalk between type I-IFNs and inflammasomes, highlighting the importance of the cross-regulation and a potential double-negative feedback loop that regulates the output of DNA-sensing pathways.

Dendritic cells and macrophages deficient in AIM2, ASC, or caspase-1 produce higher amounts of IFN-β in response to DNA transfection, which has been proposed to be due to caspase-1-dependent cell death (Corrales et al., 2016). It's conceivable that inflammasome activation-caused pyroptotic cell death would diminish type I-IFN production only if infected cells die before IFNs are produced. However, virus-induced type I-IFN production peaked between 18–24 hr post infection, whereas virus-induced pyroptosis occurred usually around 48 hr after infection (Tan and Chu, 2013; Wu et al., 2013b), especially when cells were infected at lower viral MOI. Moreover, since the enforced inflammasome activation did not affect RNA virus triggered type I-IFN production, and inflammasome activation caused similarly reduced type I-IFN production in pyroptosis-resistant *Gsdmd*$^{-/-}$ cells, it is unlikely that caspase-1-dependent pyroptotic cell death is essential in this process. In addition, iBMM cells stably expressing cGAS non-cleavable mutants showed normal inflammasome activation to either DNA or RNA virus, but enhanced type I-IFN production to DNA virus, confirming that the cleavage of cGAS accounts for the reduced cytokine production.

We found that the N-terminal fragment containing residues 120 to 160 of cGAS is critical for its normal function ex vivo. This finding is somehow surprising since previous work indicated that N terminus of cGAS from amino acids 1 to 160 was dispensable for its function when overexpressed (Sun et al., 2013), which we believed is most likely caused by overexpression. Moreover, we identified that R/K-rich region in residues 122 to 133 of h-cGAS and 119 to 132 of m-cGAS is required for cGAS activation. We propose that this positively charged region also serves as a DNA binding domain, with the help of the other one located between residues 160 and 212, to form a stable DNA-cGAS complex. In agreement with this, caspase-1 was found to cleave cGAS after this region and inactivate cGAS.

EXPERIMENTAL PROCEDURES

Mice

Casp1$^{-/-}$, *Asc*$^{-/-}$, and *Aim2*$^{-/-}$ mice backcrossed to C57BL/6 for at least 10 generations were provided by V. Dixit (Genentech). Wild-type B6 mice were purchased from Laboratory Animal Center of the Academy of Military Medical Science. Mice were kept and bred in pathogen-free conditions. All animal studies were conducted at the AAALAC approved Animal Facility in the Laboratory Animal Center of Peking University. Experiments were undertaken in accordance with the National Institute of Health Guide for Care and Use of Laboratory Animals, with the approval of Peking University Laboratory Animal Center, Beijing.

Virus Infection

Cells were infected with VACV (multiplicity of infection (M.O.I.) = 0.2), HSV-1 (M.O.I. = 0.2), SeV (M.O.I. = 0.1) for 1 hr. Then cells were washed and cultured in fresh media. For in vivo studies, age- and sex-matched groups of mice were intravenously (i.v.) or intranasally (i.n.) infected with VACV (WR strain) at 3×10^6 pfu per mouse, or intravenously (i.v.) infected with VSV at 2×10^7 pfu per mouse. Organs from inoculated animals were homogenized in 0.9% NaCl (0.1 mg of tissue/ml) and assayed for viral load by standard plaque assay on BSC-1 cells.

Luciferase Reporter Assay

293T cells (1×10^5) were seeded in 24-well plates and transfected by standard calcium phosphate precipitation method. Reporter assay was performed as previously described (Sun et al., 2009).

Type I-IFN Bioassay

Type I-IFN activity was measured as previously described (Jiang et al., 2005), with reference to a recombinant human or mouse IFN-β (R&D Systems) standard using a 2fTGH cell for human and L929 for mouse stably transfected with an IFN-sensitive (ISRE) luciferase construct.

Caspase-1-Mediated Inflammasome Activation Assay

THP-1 cells, iBMMs, or BMDM cells were seeded in 12-well plates overnight before changed with Opti-MEM, and then the cells were primed with LPS (3 μg/ml) or MALP2 (50 ng/ml) for 3 hr followed by various inflammasome ligands stimulation. For NLRP3 inflammasome activation, the cells were treated with ATP (5 mM) for 60 min, rotenone (20 μM) for 6 hr, poly (I:C) (1 μg/ml), or SeV (MOI = 0.1) for the indicated times. For AIM2 inflammasome activation, the cells were transfected with poly (dA:dT) (1 μg/ml) or infected with VACV (MOI = 0.2) for the indicated times. Culture supernatants of THP-1 or iBMM cells treated with indicated stimuli were precipitated by adding an equal volume of methanol and 0.25 volumes of chloroform. The supernatant mixtures were vortexed and then centrifuged for 10 min at 20,000 g. The upper phase was discarded and 500 mL methanol was added to the interphase. This mixture was centrifuged for 10 min at 20,000 g and the protein pellet was dried at 55°C, followed by immunoblotting analysis to detect mature IL-1β p17 in THP-1 cells and mature Casp1 p20 fragment in iBMM cells, respectively.

In Vitro Protease Cleavage Assay

Samples contain recombinant caspase protein and its substrate were incubated in caspase assay buffer (100 mM HEPES, 10% (w/v) sucrose, 0.1% (w/v) CHAPS, pH 7.0, 10 mM DTT) at 37°C for 2 hr. Reactions were stopped by boiling in 2x SDS sample buffer and samples were applied to immunoblotting.

In Vitro cGAMP Activity Assay

Perfringolysin O (PFO) protein was purified as reported (Gao et al., 2015). cGAMP from indicated cells was prepared according to the reported protocol

(Wu et al., 2013a). A total of 2 μL cGAMP was mixed with 10^6 THP-1 cells in an 8 μL reaction mixture containing 1.5 ng/μl PFO, and incubated at 30°C for 1.5 hr. Cells were lysed for further immunoblotting analysis.

Digitonin Permeabilization

Cells were treated with cGAMP in 1 mL digitonin solution (50 mM HEPES pH 7.0, 100 mM KCl, 3 mM $MgCl_2$, 0.1 mM DTT, 85 mM Sucrose, 0.2% BSA, 1 mM ATP, 0.1 mM GTP, 10 μg/ml digitonin) for 30 min at 37°C. Cells were then incubated in fresh medium for indicated times before type I-IFN bioassay and immunoblotting.

Plaque Assay for Virus Titers in Mouse Organ

VACV infectivity was quantified using BSC-1 cell monolayers. Mice infected with VACV (WR strain) were sacrificed at the indicated times. Organs from mice were collected and weighed individually. Organs were disrupted using a tissue homogenizer, frozen, and thawed three times to release the virus. Several 10-fold serial dilutions of the organ supernatant were made, added to individual wells of BSC-1 cell monolayers and incubated in a CO_2 incubator at 37°C for 1–2 days. We aspirated the medium and fixed and stained the cells with 0.1% crystal violet solution for 10 min. Plaques were counted and average counts were multiplied by the dilution factor to determine the viral titer as plaque-forming units per ml.

Statistical Analysis

Student's t test or nonparametric Mann-Whitney test was used to analyze data. Survival curves were compared using Mantel-Cox test.

SUPPLEMENTAL INFORMATION

Supplemental Information includes seven figures and Supplemental Experimental Procedures and can be found with this article online at http://dx.doi.org/10.1016/j.immuni.2017.02.011.

AUTHOR CONTRIBUTIONS

Y.W. and X.N. and Z.J. designed research; Y.W. and X.N. performed the majority of experiments; P.G. assisted in protein purification and mice experiments; and S.W., M.S., M.L., J.G., R.F, X.S., and G.M. contributed new reagents and analytical tools. Y.W., X.N., X.Z., and Z.J. analyzed the data and wrote the manuscript.

ACKNOWLEDGMENTS

We thank Drs. Vishva Dixit for gene-deficient mice, Katherine Fitzgerald for immortalized macrophages, Zhijian J. Chen for human cGAS expression vector, and Feng Shao for caspase-4/11 prokaryotic expression vectors and iBMM-*Gsdmd*$^{-/-}$ cells. We also thank Min Fang (Institute of microbiology Chinese Academy of Sciences, Beijing) for Vaccinia virus (Western Reserve strain). This work was supported by grants from the Chinese Ministry of Science and Technology (2014CB542600, 2015CC040097), and the China Natural Science Foundation (31230023, 91129000, and 81621001).

Received: August 17, 2016
Revised: December 21, 2016
Accepted: February 17, 2017
Published: March 14, 2017

REFERENCES

Ablasser, A., Bauernfeind, F., Hartmann, G., Latz, E., Fitzgerald, K.A., and Hornung, V. (2009). RIG-I-dependent sensing of poly(dA:dT) through the induction of an RNA polymerase III-transcribed RNA intermediate. Nat. Immunol. *10*, 1065–1072.

Ablasser, A., Goldeck, M., Cavlar, T., Deimling, T., Witte, G., Röhl, I., Hopfner, K.P., Ludwig, J., and Hornung, V. (2013). cGAS produces a 2′-5′-linked cyclic dinucleotide second messenger that activates STING. Nature *498*, 380–384.

Alexopoulou, L., Holt, A.C., Medzhitov, R., and Flavell, R.A. (2001). Recognition of double-stranded RNA and activation of NF-kappaB by Toll-like receptor 3. Nature *413*, 732–738.

Anand, P.K., Malireddi, R.K., Lukens, J.R., Vogel, P., Bertin, J., Lamkanfi, M., and Kanneganti, T.D. (2012). NLRP6 negatively regulates innate immunity and host defence against bacterial pathogens. Nature *488*, 389–393.

Benko, S., Magalhaes, J.G., Philpott, D.J., and Girardin, S.E. (2010). NLRC5 limits the activation of inflammatory pathways. J. Immunol. *185*, 1681–1691.

Benveniste, E.N., and Qin, H. (2007). Type I interferons as anti-inflammatory mediators. Sci. STKE *2007*, pe70.

Billiau, A. (2006). Anti-inflammatory properties of Type I interferons. Antiviral Res. *71*, 108–116.

Chen, G.Y. (2016). Regulation of the gut microbiome by inflammasomes. LID - S0891-5849(16)31034-6 (LID). http://dx.doi.org/10.1016/j.freeradbiomed.2016.11.011, [pii] ([doi].

Chin, K.C., and Cresswell, P. (2001). Viperin (cig5), an IFN-inducible antiviral protein directly induced by human cytomegalovirus. Proc. Natl. Acad. Sci. USA *98*, 15125–15130.

Chiu, Y.H., Macmillan, J.B., and Chen, Z.J. (2009). RNA polymerase III detects cytosolic DNA and induces type I interferons through the RIG-I pathway. Cell *138*, 576–591.

Civril, F., Deimling, T., de Oliveira Mann, C.C., Ablasser, A., Moldt, M., Witte, G., Hornung, V., and Hopfner, K.P. (2013). Structural mechanism of cytosolic DNA sensing by cGAS. Nature *498*, 332–337.

Corrales, L., Woo, S.R., Williams, J.B., McWhirter, S.M., Dubensky, T.W., Jr., and Gajewski, T.F. (2016). Antagonism of the STING Pathway via Activation of the AIM2 Inflammasome by Intracellular DNA. J. Immunol. *196*, 3191–3198.

Crow, M.K. (2014). Advances in understanding the role of type I interferons in systemic lupus erythematosus. Curr. Opin. Rheumatol. *26*, 467–474.

Cui, J., Zhu, L., Xia, X., Wang, H.Y., Legras, X., Hong, J., Ji, J., Shen, P., Zheng, S., Chen, Z.J., and Wang, R.F. (2010). NLRC5 negatively regulates the NF-kappaB and type I interferon signaling pathways. Cell *141*, 483–496.

Cui, J., Li, Y., Zhu, L., Liu, D., Songyang, Z., Wang, H.Y., and Wang, R.F. (2012). NLRP4 negatively regulates type I interferon signaling by targeting the kinase TBK1 for degradation via the ubiquitin ligase DTX4. Nat. Immunol. *13*, 387–395.

Fernandes-Alnemri, T., Yu, J.W., Datta, P., Wu, J., and Alnemri, E.S. (2009). AIM2 activates the inflammasome and cell death in response to cytoplasmic DNA. Nature *458*, 509–513.

Gao, P., Ascano, M., Wu, Y., Barchet, W., Gaffney, B.L., Zillinger, T., Serganov, A.A., Liu, Y., Jones, R.A., Hartmann, G., et al. (2013). Cyclic [G(2′,5′)pA(3′,5′)p] is the metazoan second messenger produced by DNA-activated cyclic GMP-AMP synthase. Cell *153*, 1094–1107.

Gao, J., Tao, J., Liang, W., Zhao, M., Du, X., Cui, S., Duan, H., Kan, B., Su, X., and Jiang, Z. (2015). Identification and characterization of phosphodiesterases that specifically degrade 3'3'-cyclic GMP-AMP. Cell Res. *25*, 539–550.

Guarda, G., Braun, M., Staehli, F., Tardivel, A., Mattmann, C., Förster, I., Farlik, M., Decker, T., Du Pasquier, R.A., Romero, P., and Tschopp, J. (2011). Type I interferon inhibits interleukin-1 production and inflammasome activation. Immunity *34*, 213–223.

Hornung, V., Ablasser, A., Charrel-Dennis, M., Bauernfeind, F., Horvath, G., Caffrey, D.R., Latz, E., and Fitzgerald, K.A. (2009). AIM2 recognizes cytosolic dsDNA and forms a caspase-1-activating inflammasome with ASC. Nature *458*, 514–518.

Ishikawa, H., and Barber, G.N. (2008). STING is an endoplasmic reticulum adaptor that facilitates innate immune signalling. Nature *455*, 674–678.

Ivashkiv, L.B., and Donlin, L.T. (2014). Regulation of type I interferon responses. Nat. Rev. Immunol. *14*, 36–49.

Jabir, M.S., Ritchie, N.D., Li, D., Bayes, H.K., Tourlomousis, P., Puleston, D., Lupton, A., Hopkins, L., Simon, A.K., Bryant, C., and Evans, T.J. (2014). Caspase-1 cleavage of the TLR adaptor TRIF inhibits autophagy and β-interferon production during Pseudomonas aeruginosa infection. Cell Host Microbe *15*, 214–227.

Jiang, Z., Georgel, P., Du, X., Shamel, L., Sovath, S., Mudd, S., Huber, M., Kalis, C., Keck, S., Galanos, C., et al. (2005). CD14 is required for MyD88-independent LPS signaling. Nat. Immunol. *6*, 565–570.

Jorgensen, I., and Miao, E.A. (2015). Pyroptotic cell death defends against intracellular pathogens. Immunol. Rev. *265*, 130–142.

Kanneganti, T.D. (2010). Central roles of NLRs and inflammasomes in viral infection. Nat. Rev. Immunol. *10*, 688–698.

Kawai, T., Takahashi, K., Sato, S., Coban, C., Kumar, H., Kato, H., Ishii, K.J., Takeuchi, O., and Akira, S. (2005). IPS-1, an adaptor triggering RIG-I- and Mda5-mediated type I interferon induction. Nat. Immunol. *6*, 981–988.

Kayagaki, N., Stowe, I.B., Lee, B.L., O'Rourke, K., Anderson, K., Warming, S., Cuellar, T., Haley, B., Roose-Girma, M., Phung, Q.T., et al. (2015). Caspase-11 cleaves gasdermin D for non-canonical inflammasome signalling. Nature *526*, 666–671.

Kötter, I., Günaydin, I., Zierhut, M., and Stübiger, N. (2004). The use of interferon alpha in Behçet disease: review of the literature. Semin. Arthritis Rheum. *33*, 320–335.

Kumar, S. (2007). Caspase function in programmed cell death. Cell Death Differ. *14*, 32–43.

Lei, Y., Wen, H., Yu, Y., Taxman, D.J., Zhang, L., Widman, D.G., Swanson, K.V., Wen, K.W., Damania, B., Moore, C.B., et al. (2012). The mitochondrial proteins NLRX1 and TUFM form a complex that regulates type I interferon and autophagy. Immunity *36*, 933–946.

Lei, G., Chen, M., Li, H., Niu, J.L., Wu, S., Mao, L., Lu, A., Wang, H., Chen, W., Xu, B., et al. (2013). Biofilm from a clinical strain of Cryptococcus neoformans activates the NLRP3 inflammasome. Cell Res. *23*, 965–968.

Levy, M., Thaiss, C.A., Zeevi, D., Dohnalová, L., Zilberman-Schapira, G., Mahdi, J.A., David, E., Savidor, A., Korem, T., Herzig, Y., et al. (2015). Microbiota-Modulated Metabolites Shape the Intestinal Microenvironment by Regulating NLRP6 Inflammasome Signaling. Cell *163*, 1428–1443.

Man, S.M., Karki, R., and Kanneganti, T.D. (2016). DNA-sensing inflammasomes: regulation of bacterial host defense and the gut microbiota. Pathog. Dis. *74*, ftw028.

Mayer-Barber, K.D., Andrade, B.B., Barber, D.L., Hieny, S., Feng, C.G., Caspar, P., Oland, S., Gordon, S., and Sher, A. (2011). Innate and adaptive interferons suppress IL-1α and IL-1β production by distinct pulmonary myeloid subsets during Mycobacterium tuberculosis infection. Immunity *35*, 1023–1034.

McIlwain, D.R., Berger, T., and Mak, T.W. (2015). Caspase functions in cell death and disease. Cold Spring Harb. Perspect. Biol. *7*, 7.

Meylan, E., Curran, J., Hofmann, K., Moradpour, D., Binder, M., Bartenschlager, R., and Tschopp, J. (2005). Cardif is an adaptor protein in the RIG-I antiviral pathway and is targeted by hepatitis C virus. Nature *437*, 1167–1172.

Miggin, S.M., Pålsson-McDermott, E., Dunne, A., Jefferies, C., Pinteaux, E., Banahan, K., Murphy, C., Moynagh, P., Yamamoto, M., Akira, S., et al. (2007). NF-kappaB activation by the Toll-IL-1 receptor domain protein MyD88 adapter-like is regulated by caspase-1. Proc. Natl. Acad. Sci. USA *104*, 3372–3377.

Moore, C.B., Bergstralh, D.T., Duncan, J.A., Lei, Y., Morrison, T.E., Zimmermann, A.G., Accavitti-Loper, M.A., Madden, V.J., Sun, L., Ye, Z., et al. (2008). NLRX1 is a regulator of mitochondrial antiviral immunity. Nature *451*, 573–577.

Nallar, S.C., and Kalvakolanu, D.V. (2014). Interferons, signal transduction pathways, and the central nervous system. Journal of interferon & cytokine research : the official journal of the International Society for Interferon and Cytokine Research *34*, 559–576.

Rathinam, V.A., Jiang, Z., Waggoner, S.N., Sharma, S., Cole, L.E., Waggoner, L., Vanaja, S.K., Monks, B.G., Ganesan, S., Latz, E., et al. (2010). The AIM2 inflammasome is essential for host defense against cytosolic bacteria and DNA viruses. Nat. Immunol. *11*, 395–402.

Rathinam, V.A., Vanaja, S.K., and Fitzgerald, K.A. (2012). Regulation of inflammasome signaling. Nat. Immunol. *13*, 333–342.

Rongvaux, A., Jackson, R., Harman, C.C., Li, T., West, A.P., de Zoete, M.R., Wu, Y., Yordy, B., Lakhani, S.A., Kuan, C.Y., et al. (2014). Apoptotic caspases prevent the induction of type I interferons by mitochondrial DNA. Cell *159*, 1563–1577.

Schneider, M., Zimmermann, A.G., Roberts, R.A., Zhang, L., Swanson, K.V., Wen, H., Davis, B.K., Allen, I.C., Holl, E.K., Ye, Z., et al. (2012). The innate immune sensor NLRC3 attenuates Toll-like receptor signaling via modification of the signaling adaptor TRAF6 and transcription factor NF-κB. Nat. Immunol. *13*, 823–831.

Seth, R.B., Sun, L., Ea, C.K., and Chen, Z.J. (2005). Identification and characterization of MAVS, a mitochondrial antiviral signaling protein that activates NF-kappaB and IRF 3. Cell *122*, 669–682.

Shi, J., Zhao, Y., Wang, Y., Gao, W., Ding, J., Li, P., Hu, L., and Shao, F. (2014). Inflammatory caspases are innate immune receptors for intracellular LPS. Nature *514*, 187–192.

Shi, J., Zhao, Y., Wang, K., Shi, X., Wang, Y., Huang, H., Zhuang, Y., Cai, T., Wang, F., and Shao, F. (2015). Cleavage of GSDMD by inflammatory caspases determines pyroptotic cell death. Nature *526*, 660–665.

Sun, W., Li, Y., Chen, L., Chen, H., You, F., Zhou, X., Zhou, Y., Zhai, Z., Chen, D., and Jiang, Z. (2009). ERIS, an endoplasmic reticulum IFN stimulator, activates innate immune signaling through dimerization. Proc. Natl. Acad. Sci. USA *106*, 8653–8658.

Sun, L., Wu, J., Du, F., Chen, X., and Chen, Z.J. (2013). Cyclic GMP-AMP synthase is a cytosolic DNA sensor that activates the type I interferon pathway. Science *339*, 786–791.

Tait, S.W., Ichim, G., and Green, D.R. (2014). Die another way–non-apoptotic mechanisms of cell death. J. Cell Sci. *127*, 2135–2144.

Takeuchi, O., and Akira, S. (2010). Pattern recognition receptors and inflammation. Cell *140*, 805–820.

Tan, T.Y., and Chu, J.J. (2013). Dengue virus-infected human monocytes trigger late activation of caspase-1, which mediates pro-inflammatory IL-1β secretion and pyroptosis. J. Gen. Virol. *94*, 2215–2220.

Tweezer-Zaks, N., Rabinovich, E., Lidar, M., and Livneh, A. (2008). Interferon-alpha as a treatment modality for colchicine- resistant familial Mediterranean fever. J. Rheumatol. *35*, 1362–1365.

Ulrichts, P., Bovijn, C., Lievens, S., Beyaert, R., Tavernier, J., and Peelman, F. (2010). Caspase-1 targets the TLR adaptor Mal at a crucial TIR-domain interaction site. J. Cell Sci. *123*, 256–265.

van Kempen, T.S., Wenink, M.H., Leijten, E.F., Radstake, T.R., and Boes, M. (2015). Perception of self: distinguishing autoimmunity from autoinflammation. Nat. Rev. Rheumatol. *11*, 483–492.

White, M.J., McArthur, K., Metcalf, D., Lane, R.M., Cambier, J.C., Herold, M.J., van Delft, M.F., Bedoui, S., Lessene, G., Ritchie, M.E., et al. (2014). Apoptotic caspases suppress mtDNA-induced STING-mediated type I IFN production. Cell *159*, 1549–1562.

Wu, J., Sun, L., Chen, X., Du, F., Shi, H., Chen, C., and Chen, Z.J. (2013a). Cyclic GMP-AMP is an endogenous second messenger in innate immune signaling by cytosolic DNA. Science *339*, 826–830.

Wu, M.F., Chen, S.T., Yang, A.H., Lin, W.W., Lin, Y.L., Chen, N.J., Tsai, I.S., Li, L., and Hsieh, S.L. (2013b). CLEC5A is critical for dengue virus-induced inflammasome activation in human macrophages. Blood *121*, 95–106.

Xu, L.G., Wang, Y.Y., Han, K.J., Li, L.Y., Zhai, Z., and Shu, H.B. (2005). VISA is an adapter protein required for virus-triggered IFN-beta signaling. Mol. Cell *19*, 727–740.

Yoneyama, M., Kikuchi, M., Natsukawa, T., Shinobu, N., Imaizumi, T., Miyagishi, M., Taira, K., Akira, S., and Fujita, T. (2004). The RNA helicase RIG-I has an essential function in double-stranded RNA-induced innate antiviral responses. Nat. Immunol. *5*, 730–737.

Zhang, L., Mo, J., Swanson, K.V., Wen, H., Petrucelli, A., Gregory, S.M., Zhang, Z., Schneider, M., Jiang, Y., Fitzgerald, K.A., et al. (2014). NLRC3, a member of the NLR family of proteins, is a negative regulator of innate immune signaling induced by the DNA sensor STING. Immunity *40*, 329–341.

Zhong, B., Yang, Y., Li, S., Wang, Y.Y., Li, Y., Diao, F., Lei, C., He, X., Zhang, L., Tien, P., and Shu, H.B. (2008). The adaptor protein MITA links virus-sensing receptors to IRF3 transcription factor activation. Immunity *29*, 538–550.